Theoretical Studies of Monosubstituted and Higher Phenyl-Substituted Octahydrosilsesquioxanes

Tingting Lin, Chaobin He,* and Yang Xiao

Institute of Materials Research and Engineering (IMRE), 3 Research Link, Singapore 117602

Received: July 15, 2003; In Final Form: October 21, 2003

The electronic and structural properties of molecules (octahydrosilsesquioxane, $H_8Si_8O_{12}$), the monosubstituted and higher phenyl-substituted octahydrosilsesquioxanes ($PhH_7Si_8O_{12}$, $Ph_2H_6Si_8O_{12}$, (Ph-Ph)$H_7Si_8O_{12}$, and $Ph_8Si_8O_{12}$), and crystals ($H_8Si_8O_{12}$ and octa(phenylsilsesquioxane) acetone solvate ($C_{48}H_{40}O_{12}Si_8{\cdot}C_3H_6O$)) have been studied using plane-wave (PW), pseudo-potential (PP), and density functional theory and the generalized gradient approximation (DFT-GGA) methods. The results show that the orbitals near the highest occupied molecular orbitals (HOMOs) and lowest unoccupied molecular orbitals (LUMOs) (inclusive) for the phenyl-substituted polyhedral oligomeric silsesquioxane clusters and crystal are localized on the phenyl functional groups, whereas for both isolated molecular and crystalline $H_8Si_8O_{12}$, the HOMO is that with the lone pair on the O atoms.

1. Introduction

Among the polyhedral oligomeric silsesquioxanes (POSSs) of a general formula $R_n(SiO_{1.5})_n$ (where n is an even number ≥ 4), those with a value of $n = 8$ are studied most extensively. They are of considerable practical and theoretical interest for optoelectronic devices, especially for light-emitting, silicon-compatible structures with three-dimensional (3D) reduced-dimension nano dots.[1,2] One of the major areas of theoretical study needed to understand the optical properties of the H−POSS and the effect of substituting the H atom by other functional groups (such as a methyl or phenyl group) is the nature of the frontier electron states, e.g., how their energies and compositions are dependent on the conformation and substituents.

The absorption or emission of ultraviolet/visible (UV/Vis) light by a molecule is dependent on electron transitions between molecular-orbital energy levels. Energy is absorbed only when the amount of energy provided matches the energy difference of two energy levels. However, the orbital energy level distribution of a molecule is much more complicated than that of an atom, which is fixed. The energy-level values of a molecule are dependent on the molecular shape, bonding, and distribution of electron density within the molecule. It is well-known that the electronic spectra of gaseous molecules may assume a very complicated structure that results from the superposition of vibrational and rotational changes on the electronic transition. In electronic spectra of liquids, solutions, and solids, the rotational structure is irresolvable and even the vibrational structure is not always resolvable. Thus, the electronic spectra consist of relatively broad bands. The shapes of a molecule in the lowest electronic state (the ground electronic state) and higher electronic states (excited electronic states) are different. In the following orbital energy calculations, for simplicity, we neglected the effect of changes in the molecule shape and the vibrational and rotational effects. The energies were evaluated at the ground-state optimized geometry.

* Author to whom correspondence should be addressed. E-mail: cb-he@imre.a-star.edu.sg.

$H_8Si_8O_{12}$ is used in molecular science as an appropriated starting molecule for synthesizing monosubstituted and higher-substituted octanuclear silasesquioxanes. This compound has been well studied through the experimental measurements and theoretical calculations. The structure and geometries of octahydrosilsesquioxane have been confirmed using a variety of experimental techniques, including X-ray diffraction (XRD),[3,4] neutron diffraction,[5] nuclear magnetic resonance (NMR),[6] and infrared (IR) and Raman spectroscopy.[7,8] The ultraviolet/photoluminescence (UV/PL) spectra of $H_8Si_8O_{12}$ and alkyl-substituted $R_8Si_8O_{12}$ have been systematically investigated by Azinoic and co-workers.[9] Their study revealed that all their investigated molecules had a similar spectral structure, which consisted of intensive absorption bands at ∼6 eV and two intensive emission bands peakings at ∼3.7 and ∼4.2 eV. Several theoretical studies, performed at both the semiempirical and ab initio levels, have clarified the electronic states of the octahydrosilsesquioxane molecule. Calzaferri et al.[10] used extensive Hückel theory to study the electronic structure of the $X_8Si_8O_{12}$ (X = H, Cl, or CH_3) and found that, among the many orbitals of $H_8Si_8O_{12}$, there is exactly one orbital of A_{2g} symmetry and the pure oxygen lone-pair orbital turns out to be the highest occupied, followed by many oxygen lone pairs, which interact very slightly with Si and X atoms. Semiempirical electronic structure calculations were performed by Early,[11] using AMPAC/AM1, and the calculated results showed that Si−O bond lengths were consistently too long (by ca. 0.1 Å) and the Si−O−Si angles are too large (by ca. 10°). Accurate determination of the Si−O bond lengths and Si−O−Si angles in these molecules requires high levels of theory, including ab initio calculations based on the Hartree−Fock (HF) approximation: Hill and Sauer[12] used the direct self-consistent field (SCF) code Turbomole and a double-ζ + polarization (DZP) basis set on the Si and H atoms, and a triple-ζ + polarization (TZP) basis set on the O atoms; Earley[13] reported the results from calculations at the 6-31G(d)//6-31G(d) level using GAMESS and Gaussian92. Currently, ab initio calculations based on density functional theory (DFT) approximations have been reported by Xiang et al.[14] (who used local and nonlocal density approxima-

10.1021/jp036044m CCC: $25.00
Published on Web 11/21/2003

tions (LDA, NLDA) and double numeric basis sets (DNP, comparable to 6-31G**) in the program package DMol), Mattori et al.[15] (using the Møller−Plesset second-order perturbation method (MP2) in Gaussian98 at B3LYP level and 6-31G** basis set), and Pasquarello et al.[16] using LDA and pseudo-potentials (PPs). Methyl silsesquioxane was investigated by Franco et al.[17] using DFT, the gradient-corrected (GGA) functional, and the DNP basis set in the DMol program. However, to our knowledge, no ab initio calculations exist in the literature for phenyl-substituted $H_8Si_8O_{12}$.

The DFT method provides an accurate, and computationally economical, way of modeling electron correlation and is now widespread in molecular electronic structure studies, particularly in large molecular systems where traditional ab initio methods are clearly too intensive computationally.

A red shift was clearly noted in the absorption spectra of POSS−$(Ph)_8$, POSS−$(Ph\text{-}Ph)_8$, POSS−$(Ph\text{-}Ph\text{-}Ph)_8$, and POSS−$(Ph\text{-}Ph\text{-}Ph\text{-}Ph)_8$, which had been synthesized in our laboratory.[18] Its trend is similar to that of the linear *p*-polyphenyl molecules, which shifts toward longer wavelengths and increases in intensity as the number of benzene rings increases, and the magnitude of the wavelength shift of the band associated with the introduction of one additional phenyl group decreases progressively as the number of benzene rings increases in the *p*-polyphenyl and λ_{max} asymptotically approaches a limited value as the length of the conjugated system increases. Here is a general rule that describes the effect of double-bond conjugation on the energy absorbed by the π system. The greater the number of conjugated multiple bonds in a compound, the longer the wavelength of the light that the compound will absorb. This translates into a smaller energy requirement for the transition from the highest occupied molecular orbital (HOMO) to the lowest unoccupied molecular orbital (LUMO).

The HOMO states of benzene (the phenyl group) are doubly degenerate π states of C 2p atomic orbitals, whose orbital lobes stand vertically on the molecular plane. The effect of molecular shape on the delocalization of π electrons can be depicted as follows: when π system is nonplanar, the electrons in the double bonds are "localized" and the excited energy is large and in the UV range, whereas when the molecule is flat and the π system is conjugated, the double bonds can be delocalized.

Our goals of this work are to determine the ground-state conformations of the monosubstituted and higher phenyl-substituted $H_8Si_8O_{12}$ molecules and to predict the variation in electronic properties with the increase in the numbers of benzene rings. Total energy calculations will be performed to optimize the molecular structural parameters, such as bond lengths and bond angles. For the optimized conformations, a trend in electronic properties will then be obtained by the analysis of molecular orbital energies, electronic density maps, and density of states (DOS) plots. In Section 2, detailed computational techniques that have been used in this study are given. The results are presented and discussed in relation to experiments and previous calculations given in Section 3. Finally, conclusions of this study are given in Section 4.

2. Methods

The present calculations were performed using density functional theory (DFT) CASTEP computer code,[19−21] using ultrasoft pseudopotentials (PPs)[22] and a plane-wave (PW) basis set with a suitable cutoff. Electronic exchange and correlation were included through the generalized gradient approximation (GGA) in the Perdew−Wang form.[23] Only valence electrons were explicitly treated and PPs were used to account for core−valence interactions. The softer PPs were essential to reduce the energy cutoff. It is expected that the minimum box size and the cutoff needed to achieve the necessary accuracy vary with the size of a molecule. A supercell is constructed by placing a molecule at the center of a box that is periodically repeated in three dimensions. Because of the large distance between adjacent molecules (the smallest distance between the outermost atom at a molecule in the three-dimensional (3D) periodicity box and the atom at its most nearby imagined molecule is ≥ 8 Å), the intermolecular interactions are negligible. The band-gap energy was estimated from the energy difference between the top of the valence band and the bottom of the conduction band. The Brillouin zone integration has been performed using only the $\boldsymbol{k} = 0$ point, which is sufficient, because of the large size of the simulation box and also because the LUMO state is well separated from the HOMO state.

3. Results and Discussions

To test the reliability of our methodology, we started by performing a geometric optimization for the $H_8Si_8O_{12}$ core molecule, because a variety of levels of ab initio calculation results and plenty of accumulated experimental data have been reported in the literature. The molecule was put in the center of a simple cubic box. Two runs were performed with different box sizes and basis set cutoffs: a supercell size of 15 Å ("Coarse") and a cutoff of 260 eV and a supercell size of 18 Å ("Fine") and a cutoff of 340 eV. A comparison of our calculation results with other theoretical results and experimental data is listed in Table 1. The optimized bond lengths (*R*) and angles are in agreement with the experimental data and are comparable to those of all electrons calculations with a big basis set (such as 6-31G**) when the supercell size and the PW basis set energy cutoff are sufficiently large. The symmetry of the optimized isolated $H_8Si_8O_{12}$ molecule is similar to O_h, whereas, in the crystal, the molecule has T_h symmetry.[5] Tornroos attributed the deviation from ideal O_h symmetry to the fact that the soft Si−O−Si angles provide flexible connections between the relatively rigid $HSiO_3$ tetrahedrons. We speculated that the nonbonded intermolecular interactions, e.g., the hydrogen bonding, might be a reason for the deformation, because the smallest O···H (the distance between an O atom and a H atom at two neighboring $H_8Si_8O_{12}$ molecules) is 2.95 Å in the crystal. In our calculations, the nearest intermolecular O···H distance is 11.0 Å and the H···H distance is 10.2 Å in the 15 Å supercell; the same distances are 14.3 and 13.5 Å, respectively, in the 18 Å supercell. Therefore, the intermolecular interactions are negligible and the obtained results can be attributed to an isolated $H_8Si_8O_{12}$ molecule. The bigger the cell is, the closer to O_h symmetry the optimized structure of $H_8Si_8O_{12}$ will be. Of course, there is a penalty. The computation cost will increase as the cell size and basis set energy cutoff increases. For our cases, the CPU time increased by a factor of 4 and the memory needed by a factor of 3. For bigger clusters, we must find a balance between the accuracy and the computation efficiency.

The optimized structure of $Ph_8Si_8O_{12}$ has low symmetry, because of the various orientations of the eight phenyl rings that are attached at the eight corner Si atoms of the Si_8O_{12} cage. The bond lengths and angles of the optimized $Ph_8Si_8O_{12}$ structure are given in Table 2 with corresponding experimental data. The average Si−C bond length is 1.827 Å and similar to the experiment data. The angles ∠Si−O−Si and ∠O−Si−O varied in larger ranges than those of $H_8Si_8O_{12}$, although their average values agree with the corresponding data obtained from crystal XRD. The box size is 18 Å. The intermolecular nearest

TABLE 1: Geometric Parameters for $H_8Si_8O_{12}$: A Comparison of Calculated and Experimental Data

	bond length (Å)		angle (°)			
methods and software	R_{Si-O}	R_{Si-H}	∠Si−O−Si	∠O−Si−O	∠O−Si−H	references and remarks
DFT GGA-PW91 ultrasoft PP−PW, CASTEP	1.599−1.607	1.451−1.455	147.8−149.3	107.0−112.2	108.6−110.2	This work. 15 Å supercell, 260 eV cutoff; within 0.1 Å, the optimized structure has O_h symmetry.
	1.598	1.449	149.1	109.1	109.8	This work. 18 Å supercell, 340 eV cutoff; the optimized structure has O_h symmetry.
X-ray diffraction	1.619	1.450	147.5	109.6	109.5	ref 3
X-ray diffraction	1.620		147.5−147.6	109.4−109.7		ref 4
neutron diffraction	1.623−1.626	1.459−1.463	147.25−147.45	109.14−109.53	109.07−109.77	ref 5
DFT LDA PP	1.620	1.510	148.6	109.4		ref 16
DFT LDA (NLDA) DNB, DMol^3	1.640 (1.680)		144.5 (144.6)	111.4 (111.3)		ref 14
HF 6-31G(d), GAMESS	1.630	1.457	149.0	109.0		ref 13
HF DZP, Turbomole	1.626		150.0			ref 12
DFT MP2 B3LYP 6-31G**, Gaussian98	1.640	1.460	148.2	109.6	109.3	ref 15

TABLE 2: Bond Lengths and Angles of the Optimized Structure for $Ph_8Si_8O_{12}$

bond length (Å)				angle (°)					
R_{SiO}	R_{SiC}	R_{CC}	R_{CH}	∠Si−O−Si	∠O−Si−O	∠O−Si−C	∠C−C−C	∠H−C−C	∠Si−C−C
Calculated[a]									
1.603−1.614	1.823−1.831	1.380−1.397	1.082−1.087	145.4−152.8	106.7−110.6	108.1−111.8	117.9−121.2	118.5−120.5	119.6−122.5
1.609	**1.827**	**1.387**	**1.085**	**149.5**	**108.8**	**110.1**	**120.0**	**119.8**	**121.0**
Experimental[b]									
1.614	1.828			149.2	109.0				

[a] Geometric optimization using CASTEP GGA-PW91, a cell size of 18 Å, and a cutoff energy of 260 eV. Values given in bold are average values. [b] From ref 24.

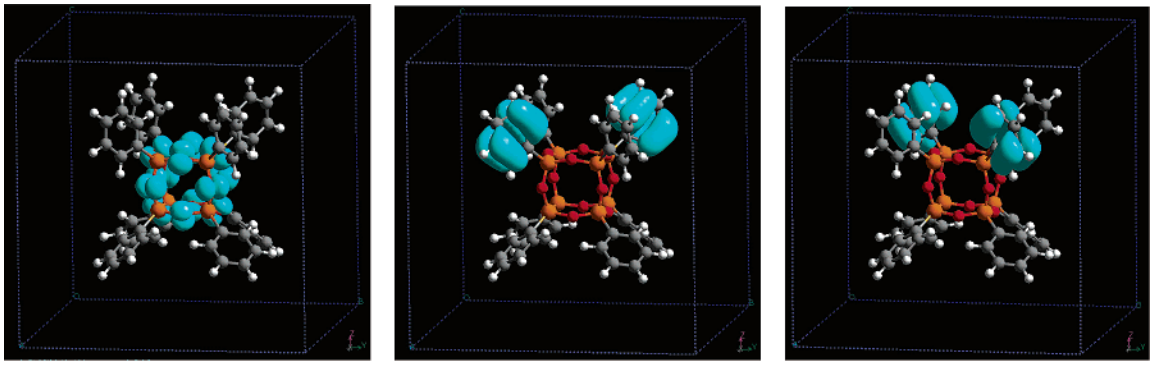

(a) (b) (c)

Figure 1. Typical orbitals of the $Ph_8Si_8O_{12}$ molecule: (a) orbital 155, showing lone pairs of electrons on O atoms; (b) orbital 168 (HOMO), depicting the π-electron orbital on phenyl groups; and (c) orbital 169 (LUMO), showing the π-electron orbital on phenyl groups.

distances of O···H and H···H are measured to be 10.8 and 7.35 Å, respectively, whereas, in the crystal,[24] the O···H bond distance is as small as 3.0 Å and the H···H bond distance is 3.1 Å between two adjacent $Ph_8Si_8O_{12}$ molecules. The cell size is not big enough for this cluster; however, it has reached our current hardware capacity limit.

The HOMO of $H_8Si_8O_{12}$ is an orbital of lone-pair electrons on O atoms. For the $Ph_8Si_8O_{12}$ molecule in the ground state, there are a total of 168 occupied (336 valence electrons) orbitals. A few typical orbitals are shown in Figure 1. All the electron charge density isosurfaces were plotted at the value of 0.01. Similar to $H_8Si_8O_{12}$, there is also one orbital (number 155) of lone-pair electrons on the O atoms. However, this orbital is lower than the HOMO (orbital 168). To get the LUMO, some empty orbitals were added. In the HOMO and LUMO (orbital 169), the electron charge density is primarily localized on the individual phenyl rings; furthermore, the orbitals resemble π-electron bonding orbitals of a free benzene molecule. Between the lone-pair orbital 155 and orbital 188 of $Ph_8Si_8O_{12}$, there are 32 π-electron orbitals on the phenyl rings: half of them are bonding and the rest are antibonding. Some of these orbitals are occupied and others are empty in the ground state.

The plots of total density of states (DOS) for some investigated molecules are illustrated in Figure 2. Comparing the DOS plots, it was obvious that the total DOS of $Ph_8Si_8O_{12}$ is a superposition of the DOS of the eight phenyl substituents and the cage. The methyl side-groups in $Me_8Si_8O_{12}$ contribute to the spectra only in the inner-valence regions, whereas the contributions of phenyl groups in $Ph_8Si_8O_{12}$ also are important in the outer valence region (near the HOMO region). There are two sharp peaks around the HOMO and LUMO in the total DOS plot of $Ph_8Si_8O_{12}$. The energies of these orbitals are very similar to HOMO or LUMO and they are of the π-electron type. As a result, the first band in the absorption spectrum is due to the transitions of electrons from the bonding π orbitals of these phenyl rings to the antibonding π orbitals. We also performed

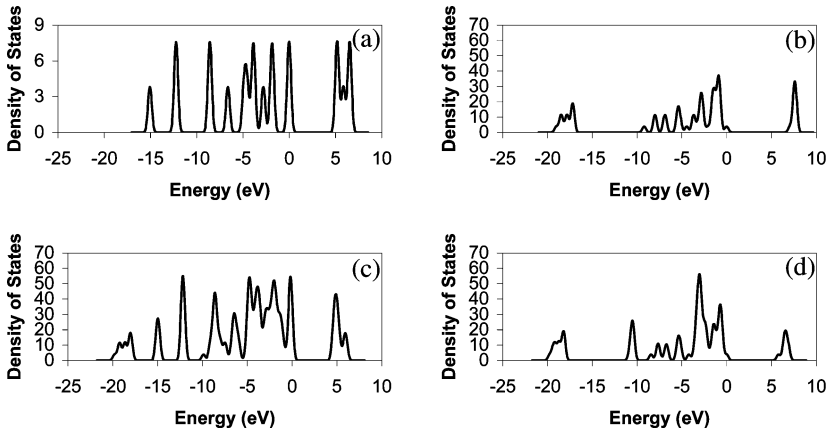

Figure 2. Total density of states (DOS) plots for the optimized structures of molecules: (a) C_6H_6 (benzene), (b) $H_8Si_8O_{12}$, (c) $(C_6H_5)_8Si_8O_{12}$ (or $Ph_8Si_8O_{12}$), and (d) $(CH_3)_8Si_8O_{12}$ (or $Me_8Si_8O_{12}$).

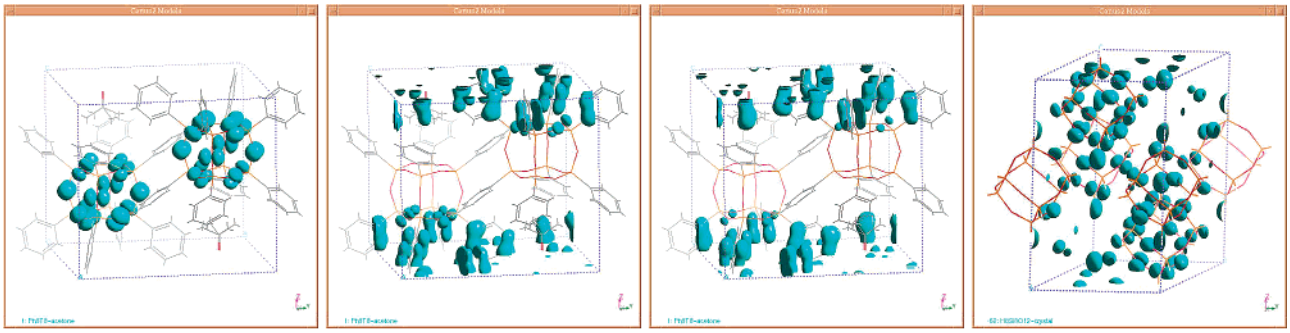

Figure 3. Some frontier orbitals, depicting (a) the crystal $Ph_8Si_8O_{12}$−acetone[24] orbital 338 (HOMO-36), (b) orbital 355 (HOMO-19), (c) orbital 373 (HOMO-1), and (d) the crystal $H_8Si_8O_{12}$[5] orbital 168 (HOMO).

TABLE 3: LUMO−HOMO Energy Gaps of POSS $H_8Si_8O_{12}$ and Its Methyl- and Phenyl-Substituted Geometry Optimization, Calculated Using CASTEP GGA-PW91

molecule formula	total number of atoms	LUMO−HOMO gap (eV)	wavelength (nm)	supercell size (Å)	plane-wave (PW) basis set cutoff (eV)	total energy (eV)
$H_8Si_8O_{12}$	28	6.848	181	15	260 (coarse)	−6279.04857
$H_8Si_8O_{12}$	28	7.066	175	18	340 (fine)	−6290.37463
$PhH_7Si_8O_{12}$	38	4.802	258	18	200 (<coarse)	−7218.00262
$(Ph\text{-}Ph)H_7Si_8O_{12}$	48	4.131	300	18	200 (<coarse)	−8212.57929
$(Ph)_2H_6Si_8O_{12}$[a]						
isomer 1	48	4.763	260	18	200 (<coarse)	−8212.65903
isomer 2	48	4.755	261	18	200 (<coarse)	−8212.84846
isomer 3	48	4.756	261	18	200 (<coarse)	−8212.98353
$Me_8Si_8O_{12}$	52	5.778	215	18	200 (<coarse)	−7726.74869
$Ph_8Si_8O_{12}$	108	4.625	268	18	200 (<coarse)	−14181.5155
$Ph_8Si_8O_{12}$	108	4.589	270	18	260 (coarse)	−14277.3305
$Ph_8Si_8O_{12}$ (calculated using DMol)	108	4.742	261	N.A.[b]	dnd	

[a] Three isomers of $(Ph)_2H_6Si_8O_{12}$ are examined in this study: in isomer 1, the two phenyl rings are neighboring; in isomer 2, the two phenyl rings are face diagonal; and in isomer 3, the two phenyl rings are body diagonal. [b] Not available.

a single-point energy calculation for the $Ph_8Si_8O_{12}$−acetone crystal that was built based on Hossain et al.'s measurements.[24] As shown in Figure 3, the orbitals near the Fermi energy are all π-electron type on the phenyl groups. This further supported the isolated $Ph_8Si_8O_{12}$ molecule calculation results.

The energy gaps between LUMO and HOMO for a series of phenyl-substituted $H_8Si_8O_{12}$ molecules have been evaluated, and the results are given in Table 3. For $H_8Si_8O_{12}$ itself, the gap is ∼7.1 eV, which is consistent with Xing's DMol calculation results.[14] The energy gaps for the three isomers of the molecule $(Ph)_2H_6Si_8O_{12}$ are almost the same, based on the calculations. A comparison of $PhH_7Si_8O_{12}$ with $(Ph\text{-}Ph)H_7Si_8O_{12}$, adding one more phenyl ring along the side chain, shows that the LUMO−HOMO gap decreases: that is, the wavelength is red-shifted. This observation is similar to that from benzene to biphenyl and the trend of our experimental results from POSS−$(Ph)_8$ to POSS−$(Ph\text{-}Ph)_8$. For $Ph_8Si_8O_{12}$, the gap is 4.6 eV, obtained from calculation using CASTEP, and 4.7 eV, obtained from a calculation using DMol[3]. The wavelength for POSS−$(Ph)_8$ is 269.5 nm in chloroform at 25 °C.[25,26] Our experimental measurement absorption peak for POSS−$(Ph)_8$ in tetrahydrofuran (THF) is located at 270 nm.[18] In regard to the UV spectra, oligoorganylsilsesquioxanes display no absorption in the spectral region beyond 180 nm. In the UV spectra of octa(vinylsilsesquioxane) and deca(vinylsilsesquioxane), a vinyl group absorption maximum is observed at 212 nm. The phenyl group absorption in the spectra of octa(vinylsilsesquioxanes) and deca(phenylsilsesquioxanes) corresponds to a maximum at 264 nm.[1]

Therefore, our calculated energy gap is in reasonable agreement with the experimental results.

4. Conclusion

We have presented the first ab initio calculation results for phenyl-substituted $H_8Si_8O_{12}$. The orbitals near the highest occupied molecular orbital (HOMO) and lowest unoccupied molecular orbital (LUMO) (inclusive) for the phenyl-substituted polyhedral oligomeric silsesquixoane (POSS) clusters and crystal are localized on the phenyl rings. Substitution of the H atoms with phenyl rings at one corner, two (three alternates), or all eight corners of $H_8Si_8O_{12}$ shows that the LUMO−HOMO gaps are almost the same; however, with the addition of one more phenyl ring along the side chain at the same corner, the LUMO−HOMO gap decreases and the wavelength is red-shifted.

References and Notes

(1) Voronkov, M. G.; Lavrentyev, V. I. *Top. Curr. Chem.* **1982**, *102*, 199.
(2) Calzaferri, G. *Tailor-Made Silicon−Oxygen Compounds: From Molecules to Materials*; Corriu, R., Jutzi, P., Eds.; Vieweg: Wiesbaden, Germany, 1996; p 149.
(3) Larsson, K. *Ark. Kemi* **1960**, *16*, 215.
(4) Auf der Heyde, T. P. E.; Burgi, H.-B.; Burgi, H.; Tornroos, K. W. *Chimia* **1991**, *45*, 38.
(5) Tornroos, K. W. *Acta Crystallogr., Sect. C: Cryst. Struct. Commun.* **1994**, *50*, 1646.
(6) Kowalewski, J.; Nisson, T.; Tornroos, K. W. *J. Chem. Soc., Dalton Trans.* **1996**, 1579.
(7) Bartsch, M.; Bornhauser, P.; Calzaferri, G.; Imhof, R. *J. Phys. Chem.* **1994**, *98*, 2817.
(8) Marcolli, C.; Laine, P.; Buhler, R.; Calzaferri, G. *J. Phys. Chem. B* **1997**, *101*, 1171.
(9) Azinovic, D.; Cai, J.; Eggs, C.; Konig, H.; Marsmann, H. C.; Veprek, S *J. Lumin.* **2002**, *97*, 40.
(10) Calzaferri, G.; Hoffmann, R. *J. Chem. Soc., Dalton Trans.* **1991**, 917.
(11) Earley, C. W. *Inorg. Chem.* **1992**, *31*, 1250.
(12) Hill, J.-R.; Sauer, J. *J. Phys. Chem.* **1994**, *98*, 1238.
(13) Earley, C. W. *J. Phys. Chem.* **1994**, *98*, 8693.
(14) Xiang, K.-H.; Pandey, R.; Pernisz, U. C.; Freeman, C. *J. Phys. Chem. B* **1998**, *102*, 8704.
(15) Mattori, M.; Mogi, K.; Sakai, Y.; Isobe, T. *J. Phys. Chem. A* **2000**, *104*, 10868.
(16) Pasquarello, A.; Hybertsen, M. S.; Car, R. *Phys. Rev. B* **1996**, *54*, R2339.
(17) Franco, R.; Kandalam, A. K.; Pandey, R.; Pernisz, U. C. *J. Phys. Chem. B* **2002**, *106*, 1709.
(18) He, C. B.; Xiao, Y.; Huang, J. C.; Mya, K. Y.; Zhang, X. H.; Lin, T. T. Quantum Confinement in Organic Light Emitting Dots, submitted for publication.
(19) CASTEP Users Guide; Accelrys, Inc.: San Diego, CA, 2001.
(20) Milman, V.; Winkler, B.; White, J. A.; Pickard, C. J.; Payne, M. C.; Akhmatskaya, E. V.; Nobes, R. H. *Int. J. Quantum Chem.* **2000**, *77*, 895.
(21) Payne, M. C.; Teter, M. P.; Allan, D. C.; Arias, T. A.; Joannopoulos, J. D. *Rev. Mod. Phys.* **1992**, *64*, 1045.
(22) Vanderbilt, D. *Phys. Rev. B* **1990**, *41*, 7892.
(23) Perdew, J. P.; Chevary, J. A.; Vosko, S. H.; Jackson, K. A.; Pederson, M. R.; Singh, D. J.; Fiolhais, C. *Phys. Rev. B* **1992**, *46*, 6671.
(24) Hossain, M. A.; Hursthouse, M. B.; Malik, K. M. A. *Acta Crystallogr. B: Struct. Sci.* **1979**, *35*, 2258.
(25) Brown, J. F.; Vogt, L. H.; Prescott, P. I. *J. Am. Chem. Soc.* **1964**, *86*, 1120.
(26) Brown, J. F.; Prescott, P. I. *J. Am. Chem. Soc.* **1964**, *86*, 1402.